The Influence of the *p*-Alkyl Substituent on the Isomerization of *o*-Quinones to *p*-Quinone Methides: Potential Bioactivation Mechanism for Catechols

Suzanne L. Iverson,[†] Li Qing Hu,[‡] Vesna Vukomanovic,[‡] and Judy L. Bolton*,[†]

Department of Medicinal Chemistry and Pharmacognosy (M/C 781), College of Pharmacy, University of Illinois at Chicago, 833 South Wood Street, Chicago, Illinois 60612-7231, and Department of Chemistry, Queen's University, Kingston, Ontario, Canada K7L 3N6

Received January 11, 1995[⊗]

Previously, we have shown that an additional bioactivation pathway for the hepatocarcinogen safrole (1-allyl-3,4-(methylenedioxy)benzene) exists which may contribute to its toxic effects: initial O-dealkylation of the methylenedioxy ring, forming the catechol, hydroxychavicol (HC, 1-allyl-3,4-dihydroxybenzene), 2-electron oxidation to the *o*-quinone (4-allyl-3,5-cyclohexadien-1,2-dione), and isomerization, forming the more electrophilic *p*-quinone methide (2-hydroxy-4-allylidene-2,5-cyclohexadien-1-one) [Bolton, J. L., Acay, N. M., & Vukomanovic, V. (1994) *Chem. Res. Toxicol.* **7**, 443–450]. In the present investigation, we explored the effects of changing π-conjugation at the 4-position on both the rate of isomerization of the initially formed *o*-quinones to the QMs and the reactivity of the quinoids formed from 4-propylcatechol (**1**), 2,3-dihydroxy-5,6,7,8-tetrahydronaphthalene (**2**), and 4-cinnamylcatechol (**3**). We selectively oxidized the catechols to the corresponding *o*-quinones or *p*-quinone methides and trapped these reactive electrophiles with glutathione (GSH). The GSH adducts were fully characterized by UV, NMR, and mass spectrometry. Microsomal incubations with the parent catechols in the presence of glutathione produced only *o*-quinone glutathione conjugates. However, if the trapping agent (GSH) was added after an initial incubation time, both *o*-quinone and *p*-quinone methide GSH conjugates were observed. The results indicate that extended π-conjugation at the *para* position enhances the rate of isomerization of the *o*-quinone to the quinone methide. Thus the half-life of the *o*-quinones decreased in the following order: the *o*-quinone of **1** > **2** > HC > **3**. In support of this, AM1 semiempirical calculations also showed the same trend: an increase in stability of the quinone methide relative to the *o*-quinone with extending π-conjugation at the 4-position. Finally, kinetic studies showed that the reactivity of the quinone methides with water increases with decreasing π-conjugation. These data provide further evidence that formation of these electrophilic quinone methides from *o*-quinones may be a general bioactivation pathway for synthetic and naturally occurring 4-alkylcatechols.

Introduction

o-Quinone[1] formation from naturally occurring catechols, phenols, or aromatic compounds in general has been invoked to explain the cytotoxic and/or genotoxic effects of several endogenous and exogenous compounds (*1*, *2*). The molecular mechanism for *o*-quinone cytotoxicity has been attributed to the alkylation of cellular macromolecules and/or redox cycling, generating reactive oxygen species which oxidize essential cellular components (Figure 1). Previously, we showed that an additional cytotoxic mechanism for the hepatocarcinogen safrole may exist involving O-dealkylation to the catechol hydroxychavicol (HC), 2-electron oxidation giving 4-allyl-*o*-quinone, and isomerization to the electrophilic HC-QM (Figure 2) (*3*). Quinone methides (QMs) are much more electrophilic than their *o*-quinone tautomers, and thus the chemistry of QMs is characterized by alkylation of cellular nucleophiles rather than redox reactions (*4*). They have not been as extensively studied as quinones, although their formation from butylated hydroxytoluene

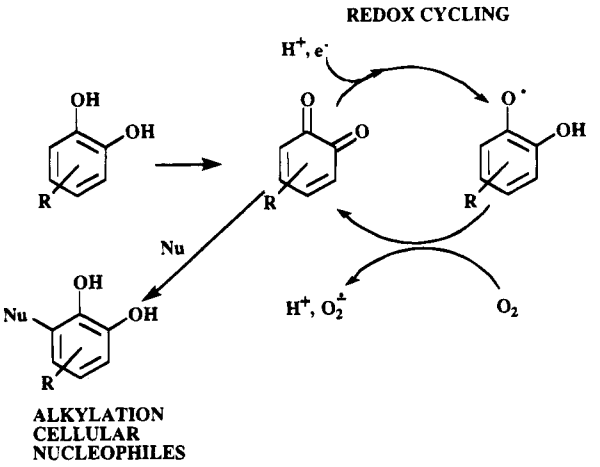

Figure 1. Oxidation of catechols to *o*-quinones and potential mechanisms of cytotoxicity.

* Address correspondence to this author at the Department of Medicinal Chemistry and Pharmacognosy (M/C 781), College of Pharmacy, University of Illinois at Chicago, 833 S. Wood St., Chicago, IL 60612-7231. FAX (312) 996-7107.
† University of Illinois at Chicago.
‡ Queen's University.
⊗ Abstract published in *Advance ACS Abstracts,* April 15, 1995.
[1] Abbreviations: P450, cytochrome P450; safrole, 1-allyl-3,4-(methylenedioxy)benzene; HC, hydroxychavicol, 1-allyl-3,4-dihydroxybenzene; QM, quinone methide, 4-alkyl-2,5-cyclohexadien-1-one, for example: HC-QM, 2-hydroxy-4-allylidene-2,5-cyclohexadien-1-one; *o*-quinone, 3,5-cyclohexadiene-1,2-dione, for example: HC-quinone, 4-allyl-3,5-cyclohexadiene-1,2-dione; BHT, butylated hydroxytoluene, 2,6-di-*tert*-butyl-4-methylphenol; eugenol, 4-allyl-2-methoxyphenol; EI-MS, electron impact mass spectrometry; CI-MS, chemical ionization mass spectrometry.

0893-228x/95/2708-0537$09.00/0

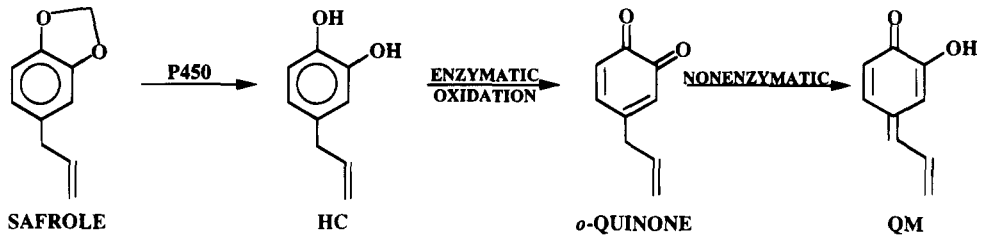

Figure 2. Cytochrome P450-catalyzed bioactivation of safrole to quinoids. Adapted from ref 3.

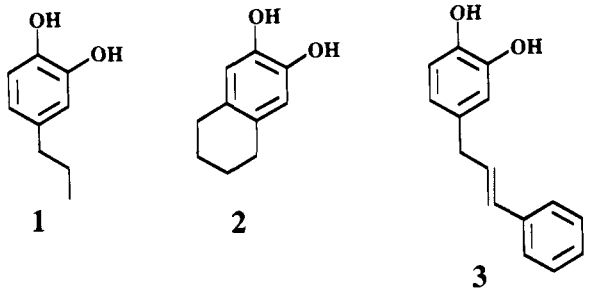

Figure 3. Structures of the 4-alkylcatechols investigated.

(BHT) and eugenol has been invoked to explain the toxicities of these food additives (*5*).

In our previous study (*3*), we selectively oxidized HC to the corresponding *o*-quinone or *p*-QM and trapped these reactive electrophiles with glutathione (GSH). The GSH adducts were fully characterized by UV, NMR, and mass spectrometry. Microsomal incubations with safrole or HC in the presence of glutathione produced only *o*-quinone glutathione conjugates. However, if the trapping agent (GSH) was added after an initial incubation of 10 min, both *o*-quinone and *p*-quinone methide GSH conjugates were observed. The first order rate constant of isomerization was estimated from the decrease in HC-quinone GSH adducts to be 1.9×10^{-3} s^{-1} ($t_{1/2}$ = 9 min). Kinetic studies showed that while HC-QM reacts rapidly with water, the model *o*-quinone (4-*tert*-butyl-3,5-cyclohexadiene-1,2-dione), which cannot isomerize to a quinone methide, was remarkably stable in aqueous solution. These results provided evidence that formation of redox-active *o*-quinones followed by isomerization to the more electrophilic QMs may be a general bioactivation pathway for 4-allylcatechols and their methylenedioxy precursors.

The present investigation concerns factors which influence the rate of cytochrome P450 (P450)-catalyzed formation of *o*-quinones, the isomerization of *o*-quinones to QMs, and reactions of the resulting QMs with nucleophiles. The catechols, shown in Figure 3, are analogs of HC with either saturated 4-alkyl substituents as in **1** and **2**, or extended π-conjugation at the *para* position as in **3**. In addition, some are metabolites of dietary aromatic ethers or analogs of carcinogenic hormones. For example, dihydrosafrole which is present in many herbs and spices, as well as insecticides, is hepatotoxic and carcinogenic in many animals (*6*). In vivo metabolic studies in the rat showed that as observed with safrole, the major metabolic pathway involves O-dealkylation of the methylenedioxy ring to give **1** (*7*). Compound **2** is an A and B ring analog of the catechol estrogen, 2-hydroxyestrone. Oxidation of the catechol estrogens to estrogen *o*-quinones and subsequent one-electron redox cycling and/or alkylation of cellular macromolecules has been proposed as the carcinogenic mechanism of these endogenous hormones (*8*). The results of this investigation suggest that the rate of isomerization of *o*-quinones to QMs and the QM hydrolysis rates are both highly dependent on the *p*-alkyl substituent, which may have a significant effect on the amount of cellular injury mediated by these electrophiles.

Materials and Methods

Materials. All chemicals were purchased from Aldrich (Milwaukee, WI), BDH (Toronto, Ontario), or Sigma (St. Louis, MO) unless stated otherwise. [^{3}H]GSH (glycine-2-^3H) was obtained from Dupont, Canada, and diluted to a specific activity of 6.0 nCi/nmol. HC was synthesized as previously described (*3*). 4-Propylcatechol (**1**) was synthesized by hydrogenation of HC. Briefly, HC (2.1 g, 14 mM) was dissolved in ethanol (50 mL), and 0.80 g of Pd on activated carbon was added along with 400 μL of trifluoroacetic acid. The flask was stirred under an H_2 atmosphere for 24 h. The solution was filtered and the solvent removed *in vacuo*. The residue was redissolved in chloroform and purified on a silica gel column with 4:1 chloroform/methanol mixture as eluant. ^{1}H NMR ($CDCl_3$) δ 0.92 (t, J = 7.3 Hz, 3H, CH_3), 1.57 (sextet, J = 7.5 Hz, 2H, CH_2), 2.47 (t, J = 7.5 Hz, 2H, benzyl CH_2), 6.61 (dd, J = 1.75 Hz, 1H, ArH^5), 6.71 (d, J = 1.71 Hz, 1H, ArH^3), 6.77 (d, J = 8.0 Hz, 1H, ArH^6); UV (CH_3CN) 228, 282 nm; positive ion CI-MS (isobutane), m/z 153 (100) (MH^+). 2,3-Dihydroxy-5,6,7,8-tetrahydronaphthalene (**2**) was synthesized from 5,6,7,8-tetrahydro-2-naphthol according to literature procedures (*9*). ^{1}H NMR ($CDCl_3$) δ 1.72 (m, 4 H, 2 × CH_2), 2.60 (m, 4 H, 2 × benzyl CH_2), 5.15 (s, 2H, 2 × OH), 6.55 (s, 2H, 2 × ArH); UV (CH_3CN) 210, 226, 288 nm; GC-MS, EI m/z 164 (75) (M). 4-Cinnamylcatechol (**3**) was synthesized by condensing catechol with cinnamic alcohol as described previously (*10*). ^{1}H NMR ($CDCl_3$) δ 3.44 (d, J = 6 Hz, 2H, CH_2), 6.38 (m, 1H, vinyl CH), 6.77 (m, 1H, vinyl CH), 7.2–7.4 (m, 8H, ArH); UV (CH_3OH) 206, 252, 284 nm; GC-MS, EI m/z 226 (100) (M).

GSH Conjugates of *o*-Quinones. The structures of the *o*-quinone GSH conjugates are shown in Figure 4. The catechols were oxidized with tyrosinase in the presence of GSH as described previously for HC (*3*). Briefly, a mixture of each catechol (5 mM), GSH (10 mM), and tyrosinase (18 900 units) in 200 mL of sodium phosphate buffer (50 mM, pH 6.0) was incubated at 25 °C for 60 min. The adducts were isolated from the aqueous phase on C-18 extraction cartridges (J. T. Baker) and eluted with methanol. The conjugates were purified by semipreparative HPLC as described below. Conjugate **4a**: ^{1}H NMR (D_2O) δ 0.93 (t, J = 7.3 Hz, 3H, CH_3), 1.56 (sextet, J = 7 Hz, 2H, CH_2), 2.16 (m, 2H, Gluβ), 2.50 (m, 2H, Gluγ), 2.75 (t, 2H, benzyl CH_2), 3.31 (m, 2H, Cysβ), 3.69 (t, J = 3.5 Hz, 2H, Glyα), 3.80 (t, J = 6 Hz, 1H, Gluα), 7.00 (s, 1H, ArH); UV (CH_3OH) 228, 276, 306 nm; positive ion electrospray-MS (1% CH_3COOH, pH 2.4), m/z 764 (26) (MH^-), 457 (26) (MH^+ − GSH). Conjugate **5a**: ^{1}H NMR (D_2O) δ 0.87 (t, J = 7 Hz, 3H, CH_3), 1.50 (sextet, J = 7.5 Hz, 2H, CH_2), 2.10 (m, 2H, Gluβ), 2.43 (m, 2H, Gluγ), 2.62 (t, J = 7 Hz, 2H, benzyl CH_2), 3.25 (m, 2H, Cysβ), 3.63 (d, J = 2.75 Hz, 2H, Glyα), 3.73 (m, 1H, Gluα), 6.82 (s, 1H, ArH^3), 7.04 (s, 1H, ArH^6); UV (CH_3OH) 210, 254, 294 nm; positive ion electrospray-MS m/z 458 (5) (MH^-), 145 (60) (Glu). Conjugate **6a**: ^{1}H NMR (D_2O) δ 0.84 (t, J = 7.3 Hz, 3H, CH_3), 1.50 (m, J = 7.4 Hz, 2H, CH_2), 2.10 (m, 2H, Gluβ), 2.41 (m, 4H, Gluγ, benzyl CH_2), 3.25 (m, 2H, Cysβ), 3.61 (d, J = 3 Hz, 2H, Glyα), 3.74 (m, 1H, Gluα), 6.74 (d, J = 1.8 Hz, 1H, ArH^3), 6.81

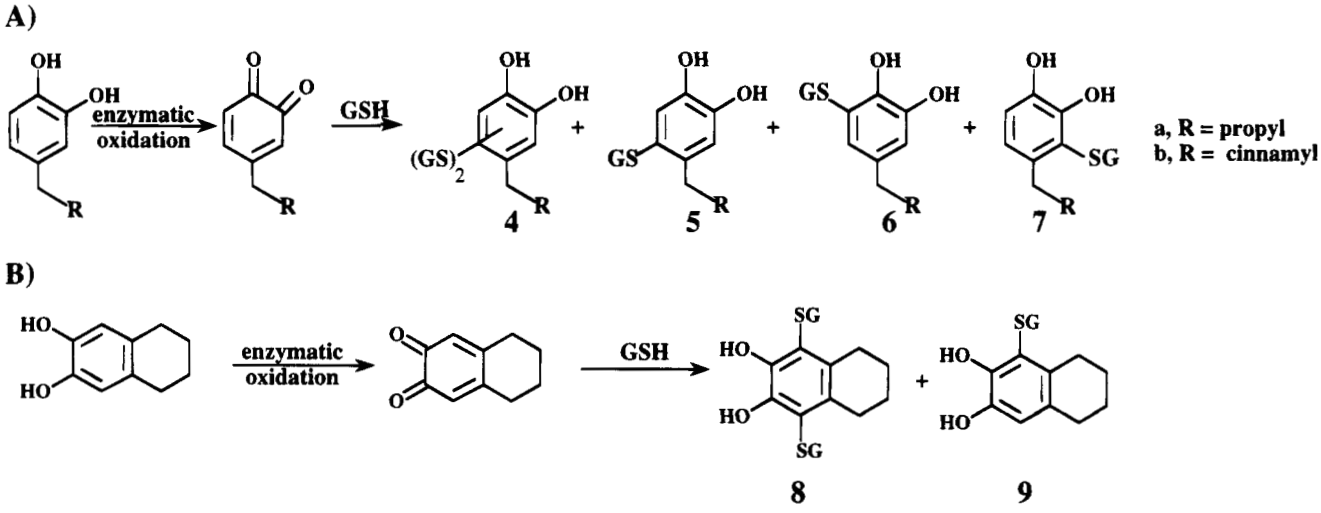

Figure 4. Structures of *o*-quinone GSH adducts. The adducts are displayed in increasing order of HPLC elution time.

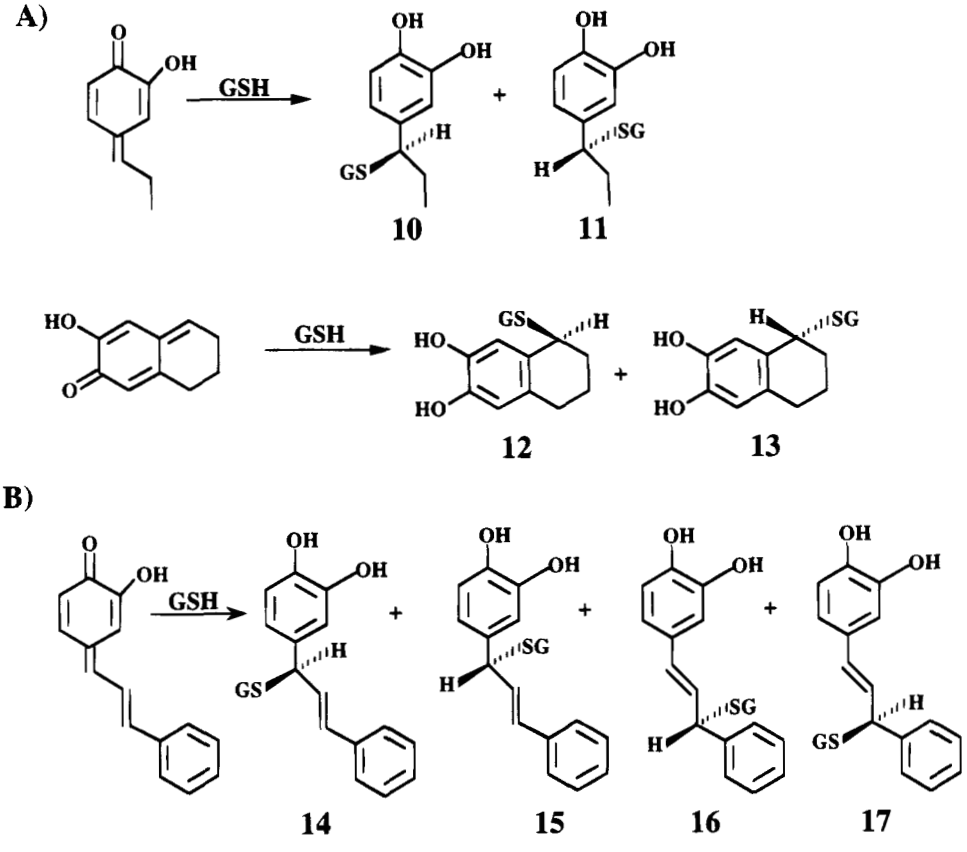

Figure 5. Structures of QM GSH adducts.

(d, J = 1.8 Hz, 1H, ArH[5]); UV (CH_3OH) 232, 256, 296 nm; positive ion electrospray-MS, m/z 458 (52) (MH^+), 145 (35) ($GluH^+$). Conjugate **7a**: ^1H NMR (D_2O, very dilute sample, only aromatic protons are reported) δ 6.66 (d, J = 8 Hz, 1H, ArH), 6.77 (d, J = 8 Hz, 1H, ArH); UV (CH_3OH) 226, 256, 296 nm; positive ion electrospray-MS, m/z 458 (15) (MH^+), 145 (90) ($GluH^+$). Conjugate **6b**: ^1H NMR (DMSO) δ 1.95 (m, 2H, Gluβ), 2.35 (m, 2H, Gluγ), 2.95 (m, 2H, Cysβ), 3.15–3.4 (m, 3H, Glyα, Gluα), 4.4 (m, 2H, Cysα, benzyl CH) 6.5 (m, 4H, 2 × ArH (catechol ring), 2 × vinyl H), 7.3 (m, 5H, ArH), 8.3 (m, 2H, 2 × OH); UV (CH_3OH) 208, 256, 295 nm; positive ion electrospray-MS, m/z 532 (55) (MH^+), 554 (30) (M + Na). Conjugate **8**: ^1H NMR (D_2O) δ 1.57 (bs, 4H, 2 × CH_2), 1.97 (m, 2H, Gluβ), 2.31 (m, 2H, Gluγ), 2.66 (bs, 4H, 2 × benzyl CH_2), 3.07 (m, 2H, Cysβ), 3.57 (m, 3H, Gluα, Glyα), 4.14 (m, 1H, Cysα); UV (CH_3OH) 220, 278, 306 nm; positive ion electrospray-MS, m/z 775 (5) (MH^+), 797 (3) (M + Na). Conjugate **9**: ^1H NMR (D_2O) δ 1.47 (bs, 4H, 2 × CH_2), 1.95 (m, 2H, Gluβ), 2.28 (m, 2H, Gluγ), 2.50 (bs, 4H, 2 × benzyl CH_2), 2.98 (m, 2H, Cysβ), 3.57 (m, 3H, Gluα, Glyα), 4.14 (m, 1H, Cysα), 6.48 (s, 1H, ArH); UV (CH_3OH) 228, 260, 302 nm; positive ion electrospray-MS, m/z 470 (100) (MH^+).

GSH Conjugates of QMs. The structures of the QM GSH conjugates are shown in Figure 5. The QMs were prepared using a modification of the procedure described for vinyl QMs (*3*, *11*). Silver oxide (5 g, 21.6 mmol) was added to 100 mg (0.7 mmol) of each catechol in 100 mL of acetonitrile and the mixture stirred for 30 min at 60 °C. The solution was filtered and added in aliquots (4 × 25 mL) to a 10 mM solution of GSH in 100 mL of potassium phosphate buffer (pH 7.4). The CH_3CN was removed after each addition under vacuum. The final concentration of the QM in the aqueous solution was 25 mM. The remaining aqueous solution was washed with ether. The adducts were isolated from the aqueous phase on C-18 extraction cartridges (J. T. Baker) and eluted with methanol. The

eluates were concentrated and subjected to semipreparative HPLC with an Ultrasphere ODS column (10 × 250 mm, Beckman) with a flow rate of 3.5 mL/min, and the same mobile-phase composition described below for analytical work. Conjugates **10** and **11**: ^{1}H NMR (D_2O) δ 0.94 (t, J = 7 Hz, 3H, CH_3), 1.30 (m, 2H, CH_2), 2.15 (m, J = 8 Hz, 2H, Gluβ), 2.52 (t, J = 6.8 Hz, 2H, Gluγ), 3.35 (m, 2H, Cysβ), benzyl CH obscured by suppression of HOD peak, 6.90 (m, 3H, ArH); UV(CH_3OH) 232, 282 nm; positive ion electrospray-MS, m/z 456 (11) (MH^+). Compound **2** could not be oxidized with Ag_2O. As a result, the QM of **2** was generated by oxidizing **2** with mushroom tyrosinase as described above. GSH was added after an initial incubation time of 30 min. Conjugates **12** and **13**: ^{1}H NMR (D_2O) δ 1.60 (m, 2H, CH_2), 1.88 (m, 2H, CH_2), 2.08 (m, 2H, Gluβ), 2.50 (m, 2H, benzyl CH_2), 3.01 (m, 1H, Cysβ), 3.50, (m, 1H, benzyl CH), 3.61 (m, 3H, Gluα, Glyα), 4.03 (m, 1H, Cysα), 6.52 (s, 1H, ArH), 6.77 (s, 1H, ArH); UV(CH_3OH) 226, 288 nm; positive ion electrospray-MS, m/z 470 (29) (MH^+). Conjugates **14**–**17**: UV (CH_3OH) 208, 266, 300 nm; positive ion electrospray-MS, m/z 532 (29) (MH^+).

Kinetic Experiments. Solvolysis experiments were conducted at 25 °C in 50 mM K_2HPO_4 (pH 7.4) (*12*). Reactions were conducted by adding 30 μL of a 3.8 mM solution of the QM from **3** in acetonitrile (0.11 mM final concentration) to 970 μL of buffer, and the first-order decay was followed by the change in absorbance at 420 nm for at least 6 half-lives with a Hewlett Packard Model 8452A diode array UV–vis spectrophotometer (*3*, *12*). All rate constants were determined in triplicate. As we were unable to generate pure solutions of the QM from **1**, the hydrolysis rate was estimated as follows. Previous work showed that replacement of an *o*-methoxy group in the QM from 4-allyl-2-methoxyphenol (eugenol-QM) by a hydroxy substituent (HC-QM) enhanced the water solvolysis rate by 2-fold (*3*). The hydrolysis rate of the QM from 2-methoxy-4-propylphenol is 0.12 s^{-1} (*13*). Thus the hydrolysis rate of the QM from **1** is predicted to be 0.24 s^{-1}.

Calculations. The energies and structures of the quinoids were obtained by geometry optimization using the AM1 Hamiltonian (*14*) as implemented in SPARTAN 3.0 (*15*) on an SGI Iris Indigo. Single point energies on the optimized geometries were calculated using *ab initio* quantum chemical calculations at the Hartree–Fock level with the 3-21G* basis set (*16*), as executed by the SPARTAN 3.0 computer program.

Incubations. Male Sprague-Dawley rats (180–200 g) were obtained from Charles River (Montreal, Quebec). Microsomes were prepared from rat liver, and protein and P450 concentrations were determined as described previously (*17*). Incubations containing 1.0 nmol of P450 were conducted for 10 min at 37 °C in 50 mM phosphate buffer (pH 7.4, 500 μL total volume). Substrates were added as solutions in dimethyl sulfoxide, and [^{3}H]GSH (specific activity of 6.0 mCi/mmol) was added in phosphate buffer, to achieve final concentrations of 0.5 and 1.0 mM, respectively. An NADPH generating system consisting of 0.4 mM $NADP^+$, 7.5 mM glucose 6-phosphate, and 1 unit/mL glucose-6-phosphate dehydrogenase was used together with 5.0 mM $MgCl_2$. For control incubations, $NADP^+$ was omitted. The reactions were initiated by the addition of $NADP^+$ and terminated by chilling in an ice bath followed by the addition of perchloric acid (25 μL).

Adduct Quantification. The incubates were centrifuged at 13 000 rpm for 6 min to precipitate microsomal protein. Aliquots of the supernatant (100 μL) were analyzed directly by HPLC with a 4.6 × 150 mm Ultrasphere C-18 column (Beckman) on a Shimadzu LC-10A gradient HPLC with an SPD-10AV UV detector set at 280 nm. The mobile phase consisted of 5% methanol in 0.25% perchloric acid/0.25% acetic acid at 1.0 mL/min for 5 min, increased to 40% CH_3OH over 45 min, isocratic for 5 min, and increased to 90% CH_3OH over the last 20 min. For quantification of GSH conjugates, 0.3 mL aliquots of the column effluent were collected during each run, and radioactivity was measured with a Beckman Model LS 5801 liquid scintillation counter. Concentrations of the GSH conjugates were calculated by summing the radioactivity associated with each peak and converting the data to nanomolar amounts using the specific activity of the [^{3}H]GSH.

Instrumentation. HPLC experiments were performed on a Shimadzu LC-10A gradient HPLC with an SPD-10AV UV detector and SIL-10A auto injector. Peaks were integrated with Shimadzu Ezchrom software and a 486-33 computer. UV spectra were measured with a Hewlett Packard Model 8452 diode array UV spectrophotometer, and ^{1}H NMR spectra were obtained with a Bruker AC-F 200 or AM 400 spectrometer at 200 or 400 MHz, respectively. Electrospray, EI, and CI mass spectra were obtained with a VG Quattro instrument. The electrospray conditions were 4 μL/min of 1% CH_3COOH (positive ion) using a Phoenix HPLC system 20.

Results and Discussion

GSH Adducts of Quinoids. Mushroom tyrosinase is known to exhibit wide substrate specificity and will readily oxidize a number of *o*-diphenolic compounds, generally producing *o*-quinones (*18*). QMs have also been reported but only in a few cases (*19*). Previously we showed that the HC-*o*-quinone is the initial product of enzymatic oxidation of HC by trapping it with GSH (*3*). In this investigation, we examined the tyrosinase-catalyzed oxidation of the catechols shown in Figure 3 in the presence of GSH. In all cases, ring-substituted GSH conjugates were produced resulting from reaction of GSH with the *o*-quinones (Figure 4). HPLC analysis of the catechol oxidation products formed in the presence of GSH indicated the formation of one major product in each case, conjugate **6** from the *o*-quinones of **1** and **3**, and conjugate **9** from the *o*-quinone of **2**. The other minor GSH conjugates are ring-substituted regioisomers (**5**, **7**) as well as di-GSH conjugates (**4**, **8**) which are analogous to the products produced from reaction of GSH with the HC-*o*-quinone (*3*). GSH would be expected to react more selectively at C-6, since this position is less sterically hindered, and the resulting anion enjoys greater resonance stabilization (*20*). It is not clear whether this is a detoxification route in vivo, because these conjugates may autoxidize at higher rates than the corresponding catechol (*21*, *22*). However, it may be argued that GSH conjugation decreases the number of electrophilic sites in the *o*-quinone and, by increasing the hydrophilicity, facilitates excretion.

In previous work, oxidation of HC with silver oxide produced a QM that was sufficiently stable in CH_3CN to allow spectral characterization (*3*). Addition of the HC-QM to GSH in aqueous solution and subsequent HPLC analysis produced three faster eluting conjugates compared to those obtained from the tyrosinase-mediated oxidation. Two of the conjugates were the diastereoisomers resulting from attack of chiral GSH at the prochiral benzyl carbon of the HC-QM. The slower eluting adduct was identified as the trans adduct resulting from 1,8-addition of GSH at the 3′-position of HC-QM. In contrast to the HC results, oxidation of **1** with silver oxide gave mainly *o*-quinone derived GSH adducts; however, enough of the diastereoisomeric QM GSH conjugates (**10**, **11**, Figure 5) were produced to allow spectral characterization. It is likely that the *o*-quinone of HC is also the initially formed oxidation product which rapidly isomerizes to HC-QM in acetonitrile. Isomerization of the *o*-quinone to the QM only slowly occurs during silver oxide-mediated oxidation of **1** because this QM is not stabilized by extended π-conjugation (see below). As we were unable to oxidize **2** with silver oxide, we generated the corresponding QM through oxidation of **2** with

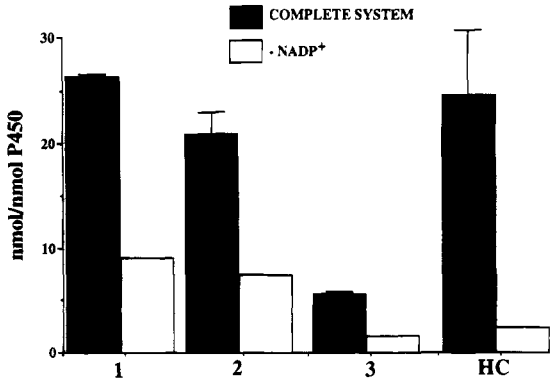

Figure 6. o-Quinone GSH conjugates produced in rat liver microsomal incubations in the presence of an NADPH generating system and 1.0 mM GSH after 10 min at 37 °C. Results are the mean ±SD of three determinations (black bars). White bars show P450-independent oxidation.

tyrosinase in the absence of GSH to allow the initially formed o-quinone to isomerize to the QM. GSH was added after 30 min, and as with **1**, two diastereoisomeric QM GSH conjugates (**12**, **13**, Figure 5) were identified and fully characterized. Oxidation of **3** with silver oxide gave the expected QM (λ_{max} = 404 nm, CH_3CN) which reacted with GSH to give four GSH conjugates (**14**–**17**, Figure 5). As the conjugates have very similar chromatographic properties, attempts to separate the conjugates from each other were unsuccessful.

Oxidation of Catechols by Cytochrome P450. We examined the oxidation of the catechols to quinoid metabolites in rat liver microsomes by trapping these reactive species with [^{3}H]GSH (*12*). The trapping reaction should be very efficient due to the high concentration of GSH in the medium, and the relatively fast rate of addition of thiols to quinoids relative to amino or hydroxyl groups (*23*, *24*). For example, the pseudo-first-order rate of addition of GSH to 4-methyl-o-quinone is 1.2×10^2 s^{-1}, which was 3–4 orders of magnitude greater than non-sulfhydryl containing nucleophiles (*25*). Nevertheless, a small amount of binding to microsomal protein is possible, so conjugate formation shown in Figure 6 is a lower limit for the generation of quinoids. The radiochromatograms gave peaks with retention times and UV spectra identical to those derived from addition of GSH to the o-quinones (data not shown); QM derived GSH adducts were not observed under these experimental conditions as the rate of trapping of the o-quinone by GSH is much faster than the rate of isomerization of the o-quinone to the QM. Quantitative data for metabolism of the catechols **1**, **2**, and HC showed that similar amounts of o-quinone GSH conjugates were produced (Figure 6). All three catechols have similar lipophilic properties, which may explain why little P450-catalyzed regioselectivity is observed. Catechol **3** gave approximately 4-fold less o-quinone derived adducts possibly due to the limited size of the active site of the particular P450 isozyme responsible for the transformation. Alternatively, the observed differences in product formation may also be due to variable o-quinone-mediated inhibition of further P450-catalyzed π-oxidation as quinones can interfere with the electron supply to the hemoprotein by accepting electrons directly from P450 reductase (*26*). o-Quinone GSH conjugates were also observed in catechol incubations in the absence of NADPH. These results indicate that the majority of 2-electron oxidation is mediated by P450; however, the reduced amount of o-quinone derived GSH products in the control incubations suggests that an additional oxidation mechanism(s) not involving P450s may be involved in the metabolism of these catechols.

Table 1. Rates of o-Quinone Disappearance and QM Hydrolysis

	half-life (min)	
catechol	rate of o-quinone disappearance[a]	QM hydrolysis[b]
1	89	0.05[c]
2	20	ND[d]
HC[e]	9	5.6
3	3	45

[a] **1** was oxidized by silver oxide in acetonitrile, and incubations were conducted by adding acetonitrile solutions of the o-quinone (0.5 mM final concentration) to phosphate buffer. **2** (0.5 mM) was oxidized by mushroom tyrosinase in the absence of GSH, extracted with ether, exchanged with acetonitrile, and added back to phosphate buffer. Due to the fast rate of isomerization, **3** (0.5 mM) was oxidized by mushroom tyrosinase in the absence of GSH without ether extraction. For all catechols, incubations (15 mL) were conducted at 25 °C (pH 6.0). Aliquots (500 μL) were combined with 5.0 mM GSH at various times. The sum of the peak area ratios of the o-quinone GSH conjugates was plotted against time, and the first-order decay was used to calculate the half-life of the o-quinone. [b] Reactions were conducted by adding acetonitrile solutions of each QM (0.1 mM final concentration) to phosphate buffer (pH 7.4) at 25 °C, and the disappearance of the reactant was determined at the λ_{max}. Results are the means of 3 determinations. [c] Estimate based on the solvolysis rate of the QM from 2-methoxy-4-propylphenol as described in Materials and Methods. [d] Not determined. [e] Data from ref 3.

Isomerization of the o-Quinones to p-QMs. Once the stores of intracellular GSH have been depleted, isomerization of the o-quinone to the p-QM could occur, resulting in a potent electrophile which could potentially alkylate numerous biopolymers, including proteins (*27*) and nucleic acids (*28*). Enzyme-catalyzed QM formation from o-quinones has been proposed to account for the sclerotization process in insect cuticle and melanization in mammals (*5*, *29*). The extreme reactivity of these QMs is used to the host cell's advantage by reacting with themselves or macromolecules in cells to generate the highly polymerized, complex structures of cuticle or melanin. For example, *N*-acetyldopamine is oxidized by cuticular enzyme(s) to an o-quinone which isomerizes to the p-QM, catalyzed by quinone isomerase (*30*, *31*). Simple catechols such as 4-methylcatechol are also oxidized to o-quinones which isomerize to QMs catalyzed by cuticular polyphenol oxidase (*19*).

Previously we showed that the o-quinone of HC was the initially formed kinetic product which isomerized to the thermodynamically more stable QM intermediate over time (*3*). In contrast to the sclerotization or melanization mechanisms, however, the isomerization of the o-quinone to its QM tautomer was not enzyme-catalyzed. Thus, incubation of HC with tyrosinase, ether extraction to separate the incubate from the enzyme, addition to pH 6.0 buffer, and quenching with GSH at various times showed a decrease in o-quinone GSH adducts along with the appearance of the GSH conjugates resulting from trapping of the HC-QM. The first-order rate constant of isomerization was estimated from the decrease in o-quinone GSH adducts to be 1.9×10^{-3} s^{-1} ($t_{1/2}$ = 9 min). In the present study, we have shown that a similar process occurs with catechols **1**–**3**; oxidation with either tyrosinase or silver oxide followed by quenching with GSH at various times also yielded a time-dependent decrease in o-quinone GSH adducts (Table 1, Figure 7).

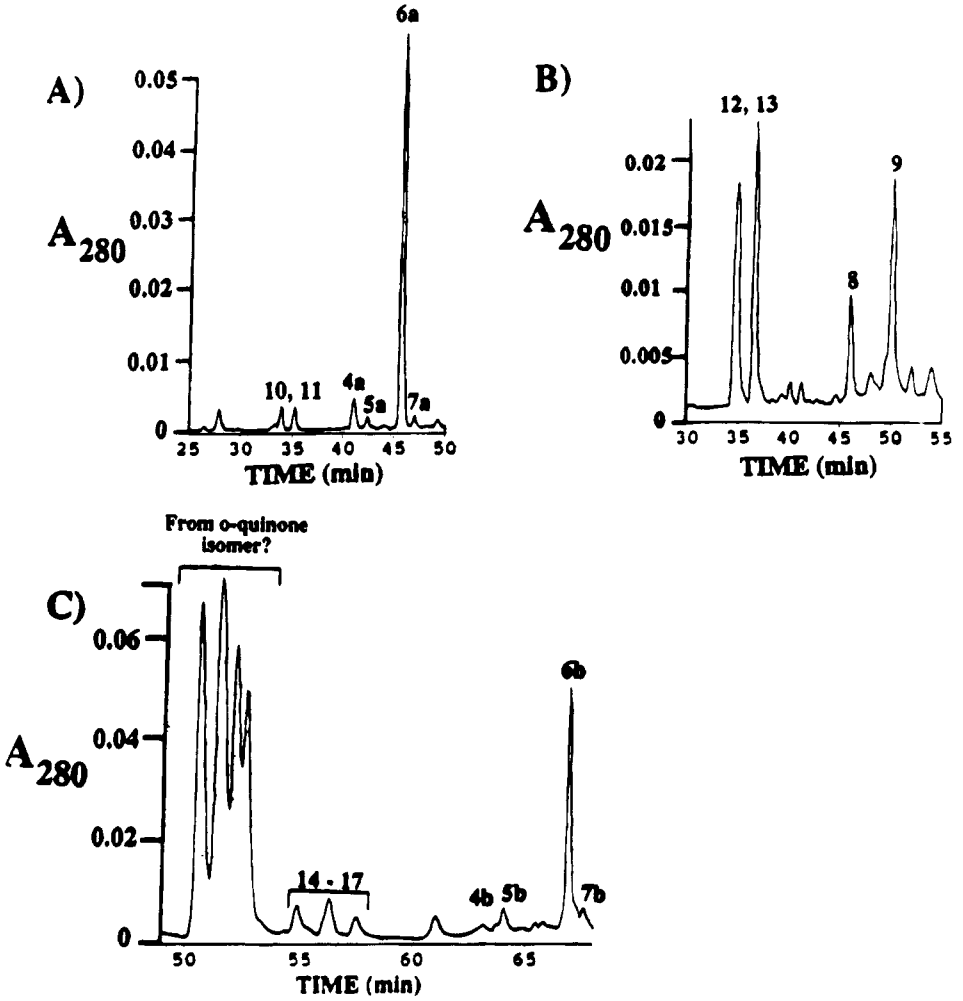

Figure 7. HPLC chromatograms of incubations conducted with catechols **1**–**3** and mushroom tyrosinase, followed by addition of 5 mM GSH. (A) **1**, GSH added after 10 min. (B) **2**, GSH added after 60 min. (C) **3**, GSH added after 10 min.

The *o*-quinone of **1** had the slowest rate of disappearance ($t_{1/2}$ = 89 min). The ring-substituted analog from **2** isomerized at 4 times the rate, perhaps due to the statistical increase in benzyl hydrogens and the existence of optimum geometry for the isomerization reaction imposed by the ring. With the *o*-quinone of **3**, a complex pattern emerged (Figures 7C and 8). The *o*-quinone GSH conjugates disappeared rapidly with a corresponding increase in earlier eluting peaks which may be the result of reaction of GSH with a structural isomer of the *o*-quinone in which the double bond has moved in conjugation with the quinone ring (Figure 8, middle structure). During the synthesis of **3**, it was observed that the catechol could not be purified by flash chromatography due to a similar, presumably acid-catalyzed, isomerization of **3** to 1-(3,4-dihydroxyphenyl)-3-phenylpropene. The rate of appearance of the QM GSH adducts correlated with the rate of disappearance of the intermediate peaks. Attempts were made to characterize these four unidentified adducts; however, purification was impossible due to the similar chromatographic properties of the conjugates. The lifetimes of the *o*-quinones of **3** were estimated from the pseudo-first-order rate of disappearance of the GSH trapped products by HPLC (Figure 8), whereas the reactivity of the QM of **3** was determined spectrophotometrically as described in Table 1.

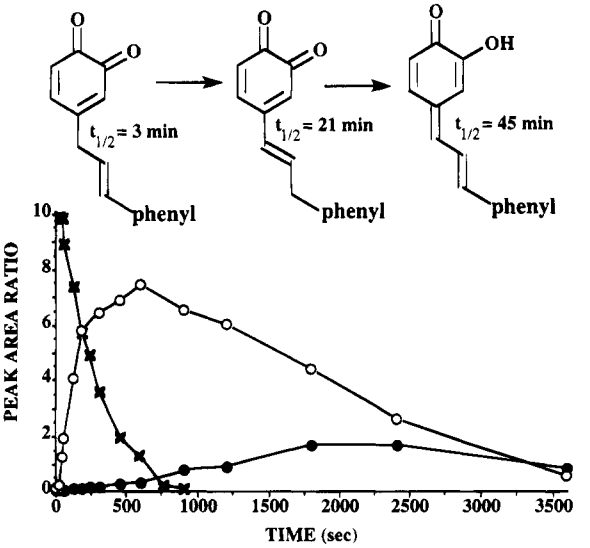

Figure 8. Oxidation of **3** by mushroom tyrosinase: effect of combining with GSH at various times. Incubations were conducted for 120 min, 25 °C, pH 6.0. At various times 500 μL of the incubate was added to 5.0 mM GSH. (×) *o*-quinone GSH conjugates (**4b**–**7b**), (●) QM GSH conjugates (**14**–**17**), (○) tentatively identified as *o*-quinone GSH conjugates from the structural isomer (middle structure) shown in the figure.

Reactivity of QMs. Rate data for the hydrolysis of the QMs compared with the isomerization rates of the *o*-quinones are shown in Table 1. The hydrolysis rate of the QM from **1** is predicted to be 0.24 s^{-1}, which suggests that the additional vinyl substituent in HC-QM decreases

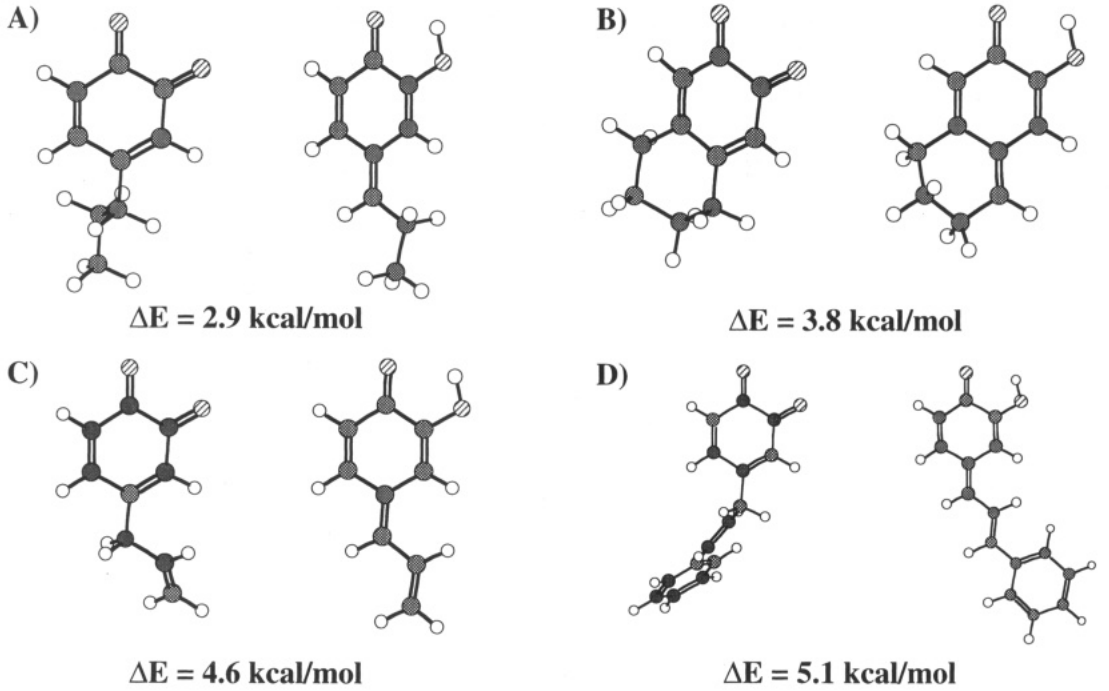

Figure 9. Minimum energy structures of the quinoids calculated at the AM1 level. ΔE represents $E_{o\text{-quinone}} - E_{QM}$. Atom symbols are (hatched circles) oxygen; (dark circles) carbon; (open circles) hydrogen. Quinoids are from (A) **1**, (B) **2**, (C) HC, (D) **3**.

the QM reaction rate by 2 orders of magnitude. The phenyl ring also imparts a modest increase on QM stability as shown by the 8-fold decrease in reactivity of the QM from **3** compared to HC-QM. As expected, the QM reactivity trend is the opposite to the *o*-quinone isomerization data where increasing π-conjugation enhanced the rate of *o*-quinone isomerization to QMs.

Calculated Energy Differences for Quinoids. In order to further investigate the effect of structure on the relative ability of *o*-quinones to isomerize to QMs, we optimized the *o*-quinone and QM structures using AM1 semiempirical calculations. Figure 9 shows the minimized structures and the energy differences between the quinoids. The minimum energy structure for all of the QMs is a planar molecule through the π-system with the hydroxyl substituent hydrogen-bonded to the oxo group. It is not known precisely the effect of an *o*-hydroxyl substituent on QM reactivity; however, we previously demonstrated that the reactivity of the QM from BHT is greatly enhanced by hydroxylation of a *tert*-butyl group (*12*). Evidence demonstrates that this effect is due to intramolecular hydrogen bonding between the ring carbonyl oxygen and the side-chain OH group which stabilizes the aromatic charge-separated resonance form. The calculated energy differences ($E_{o\text{-quinone}} - E_{QM}$) follow the same trend as the kinetic *o*-quinone isomerization data, which shows that the rate of isomerization of the *o*-quinones to the QMs heavily depends on the stability of the QM product. QMs stabilized by extended π-conjugation such as HC-QM and the QM from **3** are rapidly formed from their *o*-quinone tautomers. In contrast, only small amounts of the QM from **1** are produced from the *o*-quinone since AM1 semiempirical calculations indicate that the 4-propyl substituent does little to stabilize this QM relative to the *o*-quinone. Locking the *o*-quinone in a ring as in the *o*-quinone from **2** does enhance the rate of isomerization to the QM because of symmetry in the molecule and the favorable geometry for the reaction. As **2** is an A B ring analog of 2-hydroxyestrone and 2-hydroxyestradiol, these results indicate that this pathway may be involved in the mechanism of action of these carcinogenic endogenous steroids.

In conclusion, data have been presented on the bioactivation of catechols to *o*-quinones which isomerize to highly electrophilic *p*-QMs. The rate of isomerization depends heavily on the relative stability of the QM products; the more the QM is stabilized by extended π-conjugation in the 4-position, the faster the rate of isomerization. In this in vitro investigation, the isomerization reaction was not enzyme-catalyzed, although it is quite possible that the rate could be enhanced by enzymes such as quinone isomerase in vivo especially for catechols with saturated 4-alkyl substituents. Finally, the implications for the *o*-quinone/*p*-QM pathway in the toxicological properties of the catechols is at present unknown; however, these in vitro data suggest that this process could occur in vivo for a wide range of synthetic and naturally occurring catechols.

Acknowledgment. This research was supported by NIH Grant ES06216, NSERC Grant WFA0122931, and the University of Illinois at Chicago.

References

(1) Monks, T. J., Hanzlik, R. P., Cohen, G. M., Ross, D., and Graham, D. G. (1992) Contemporary issues in toxicology: Quinone chemistry and toxicity. *Toxicol. Appl. Pharmacol.* **112**, 2–16.
(2) O'Brien, P. J. (1991) Molecular Mechanisms of Quinone Cytotoxicity. *Chem.-Biol. Interact.* **80**, 1–41.
(3) Bolton, J. L., Acay, N. M., and Vukomanovic, V. (1994) Evidence that 4-allyl-*o*-quinones spontaneously rearrange to their more electrophilic quinone methides: Potential bioactivation mechanism for the hepatocarcinogen safrole. *Chem. Res. Toxicol.* **7**, 443–450.
(4) Powis, G. (1987) Metabolism and reactions of quinoid anticancer agents. *Pharmacol. Ther.* **35**, 57–162.
(5) Thompson, D. C., Thompson, J. A., Sugumaran, M., and Moldeus, P. (1992) Biological and toxicological consequences of quinone methide formation. *Chem.-Biol. Interact.* **86**, 129–162.
(6) *IARC Monographs on the Evaluation of Carcinogenic Risk of Chemicals to Man: Safrole, Isosafrole, and Dihydrosafrole* (1976) pp 231–244, International Agency for Research on Cancer, Lyon, France.

(7) Klungsoyr, J., and Scheline, R. R. (1982) Metabolism of isosafrole and dihydrosafrole in the rat. *Biomed. Mass Spectrom.* **9**, 323–329.
(8) Liehr, J. G. (1990) Genotoxic effects of estrogens. *Mutat. Res.* **238**, 269–276.
(9) Nutter, L. M., Ngo, E. O., and Abul-Hajj, Y. J. (1991) Characterization of DNA damage induced by 3,4-estrone-o-quinone in human cells. *J. Biol. Chem.* **266**, 16380–16386.
(10) Benson, M., and Jurd, L. (1984) Carbon-13 NMR of quinone methides. *Org. Magn. Reson.* **22**, 86–89.
(11) Zanorotti, A. (1985) Synthesis and reactivity of vinyl quinone methides. *J. Org. Chem.* **50**, 941–945.
(12) Bolton, J. L., Sevestre, H., O. Ibe, B., and Thompson, J. A. (1990) Formation and reactivity of alternative quinone methides from butylated hydroxytoluene: Possible explanation for species-specific pneumotoxicity. *Chem. Res. Toxicol.* **3**, 65–70.
(13) Bolton, J. L., Comeau, E., and Vukomanovic, V. (1995) The influence of 4-alkyl substituents on the formation and reactivity of 2-methoxy-quinone methides: Evidence that extended π-conjugation dramatically stabilizes the quinone methide formed from eugenol. *Chem.-Biol. Interact.* (in press).
(14) Dewar, M. J. S., Zoebish, E. G., Healy, E. F., and Stewart, J. J. P. (1985) AM1: A new general purpose quantum mechanical molecular model. *J. Am. Chem. Soc.* **107**, 3902–3909.
(15) Spartan v. 3.0. Wavefunction, Inc., 18401 Von Karmann, #210, Irvine, CA 92715.
(16) Pietro, W. J., Francl, M. M., Hehre, W. J., DeFrees, D. J., Pople, J. A., and Binkley, J. S. (1982) Self-consistent molecular orbital methods. 24. Supplemented small split-valence basis sets for second-row elements. *J. Am. Chem. Soc.* **104**, 5039–5048.
(17) Thompson, J. A., Malkinson, A. M., Wand, M. D., Mastovich, S. L., Mead, E. W., Schullek, K. M., and Laudenschlager, W. G. (1987) Oxidative metabolism of butylated hydroxytoluene by hepatic and pulmonary microsomes from rats and mice. *Drug Metab. Dispos.* **15**, 833–840.
(18) Passi, S., and Nazzaro-Porro, M. (1981) Molecular basis of substrate and inhibitory specificity of tyrosinase: phenolic compounds. *Br. J. Dermatol.* **104**, 659–665.
(19) Sugumaran, M., and Lipke, H. (1983) Quinone methide formation from 4-alkylcatechols: a novel reaction catalyzed by cuticular polyphenol oxidase. *FEBS Lett.* **155**, 65–68.
(20) Chardarian, C. G., and Castagnoli, N. (1979) Synthesis, redox characteristics, and in vitro norepinephrine uptake inhibiting properties of 2-(2-mercapto-4,5-dihydroxyphenyl)ethylamine (6-mercaptodopamine). *J. Med. Chem.* **22**, 1317–1322.
(21) Brunmark, A., and Cadenas, E. (1990) Biological implications of the nucleophilic addition of glutathione to quinoid compounds. In *Glutathione: Metabolism and physiological functions* (Vina, J., Eds.) pp 279–294, CRC Press, Boca Raton.
(22) Monks, T. J., and Lau, S. S. (1992) Toxicology of quinone-thioethers. *Crit. Rev. Toxicol.* **22**, 243–270.
(23) Bolton, J. L., Valerio, L. G. J., and Thompson, J. A. (1992) The enzymatic formation and chemical reactivity of quinone methides correlate with alkylphenol-induced toxicity in rat hepatocytes. *Chem. Res. Toxicol.* **5**, 816–822.
(24) Kalyanaraman, B., Premovic, P. I., and Sealy, R. C. (1987) Semiquinone anion radicals from addition of amino acids, peptides, and proteins to quinones derived from oxidation of catechols and catecholamines: An ESR stabilization study. *J. Biol. Chem.* **262**, 11080–11087.
(25) Tse, D. C. S., McCreery, R. L., and Adams, R. N. (1976) Potential oxidative pathways of brain catecholamines. *J. Med. Chem.* **19**, 37–40.
(26) Cummings, S. W., and Prough, R. A. (1983) Butylated hydroxyanisole-stimulated NADPH oxidase activity in rat liver microsomal fractions. *J. Biol. Chem.* **258**, 12315–12319.
(27) Bolton, J. L., Le Blanc, J. C. Y., and Siu, K. W. M. (1993) Reaction of quinone methides with proteins: Analysis of myoglobin adduct formation by electrospray mass spectrometry. *Biol. Mass Spectrom.* **22**, 666–668.
(28) Egholm, M., and Koch, T. H. (1989) Coupling of the anthracycline antitumor drug menogaril to 2′-deoxyguanosine through reductive activation. *J. Am. Chem. Soc.* **111**, 8291–8293.
(29) Sugumaran, M. (1991) Molecular mechanisms for mammalian melanogenesis: Comparison with insect cuticular sclerotization. *FEBS Lett.* **293**, 233–239.
(30) Saul, S. J., and Sugumaran, M. (1989) o-Quinone/quinone methide isomerase: a novel enzyme preventing the destruction of self-matter by phenoloxidase-generated quinones during immune response in insects. *FEBS Lett.* **249**, 155–158.
(31) Sugumaran, M., Saul, S. J., and Semensi, V. (1988) On the mechanism of formation of N-acetyldopamine quinone methide in insect cuticle. *Arch. Insect Biochem. Physiol.* **9**, 269–281.

TX9500033